

MACHINE LEARNING-ENHANCED INFRARED IMAGING FOR TEMPERATURE ANOMALY DETECTION IN POWER SUPPLIES *

O. Mohsen[†], M. Borland, Y.Sun Argonne National Laboratory, Lemont, IL, USA
 I. Lobach, Brookhaven National Laboratory, Upton, NY, USA

Abstract

The performance of particle accelerators is critically dependent on the reliability of their power supplies, which can number in the thousands in many facilities. In this work, we present different methods for monitoring temperature anomalies in power supplies. By applying various machine learning algorithms to the obtained features, we develop a reliable anomaly detection system that can improve the uptime of accelerator facilities. This approach enables early detection of potential issues, facilitating predictive maintenance and enhancing overall operational efficiency.

INTRODUCTION

Most accelerator facilities use power supplies to control magnets. Depending on the size of the facility, these power supplies can be numbered in the thousands. For instance, the Advanced Photon Source Upgrade (APS-U) storage ring (SR) [1], which was recently commissioned [2], uses approximately 1300 power supplies of various types to control its magnets. Earlier data from the APS indicates that the average downtime due to power supply failure was about two hours [3]. Such downtime disrupts the operation of the dozens of beamlines operating at any time. Faults in power supplies can range from equipment failure to faults caused by nuisance trips. For most of the failures in the power supplies, the stored beam is lost. In this work, we use a power supply test stand to study temperature anomalies in power supplies. Specifically, we focus on bipolar type, fast-corrector power supplies [4]. These power supplies control the corrector magnets, which are used for orbit feedback.

First, we discuss the use of an infrared (IR) camera coupled with a Machine Learning (ML) model to record and predict temperature distribution inside a power supply. We follow the work of [5], which showed promising results of using an IR camera to predict temperature anomalies using analytical methods. We discuss scalability and issues with our ML model. Moreover, we discuss the results of a larger data training study that involved all the fast correctors in one sector of the SR. Finally, we discuss the future outlook for such a model and its application to APS-U operation.

EXPERIMENTAL SETUP

To investigate the use of different diagnostics and allow flexible data acquisition, a power supply test stand was set up; see Fig. 1. The test stand can host and control different types of power supplies independently of beam operation.

* The work is supported by the U.S. DOE Office of Science-Basic Energy Sciences, under Contract No. DE-AC02-06CH11357.

[†] omohsen@anl.gov

The setup has a power supply controller, a resistive load, and several external sensors to record ambient temperature. The power supply top lid is open so that an IR camera located above the power supply can image temperature variation in the unit. The IR camera SEEK THERMAL CAMERA has a resolution of 320 x 240 pixels and is able to record images at a rate of 9 frames per second [6]. The setup has 2 independent relays that can turn on and off the power supply fans. This allows us to create synthetic anomalies by turning off a fan. Finally, a RASPBERRY PI is used to facilitate data acquisition and host the related EPICS variables on the network.

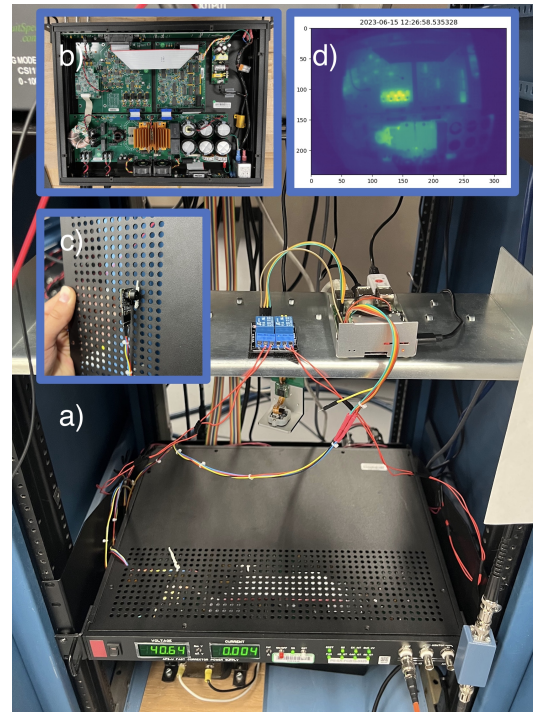


Figure 1: Power supply setup for data collection (a), the power supply test unit when the top lid is removed (b), IR camera (c) and the image obtained from the IR camera (d).

Data Collection and Processing

For all the models referenced in this work, data collection is performed over three days and then separated into three different categories: training, validation, and testing. Unlike the training and validation data, only the testing data contains synthetic anomalies, which are used to evaluate the model performance. The data used for the model consists of a series of current ramps that are generated using a pseudo-random number generator. The current $I(A)$ is varied at 1 Hz rate from -15 A to 15 A. The data from all the power supply

sensors as well as the external sensors and the IR camera are sampled at the same rate. Once the data is collected, it is processed to remove spikes in the temperature T and current. For the temperature, a moving average is applied to smooth the data, while for the current, a short median filter is applied to remove random, mostly bogus, spikes in the current while maintaining the behavior. Finally, the training data is scaled using a min-max scaler. The training scaler is used to scale both the validation and testing data.

The data from the IR camera is processed to remove barrel distortion as well as adding an average block to downsize the IR camera data from 360x240 into 8x8 pixels; see Fig. 2. We refer to the temperature of each pixel of the 8x8 image $T_{i,j}$ by its location from the top i and from the left j . Moreover, we estimate the room temperature by averaging all the pixels outside the power supply boundary.

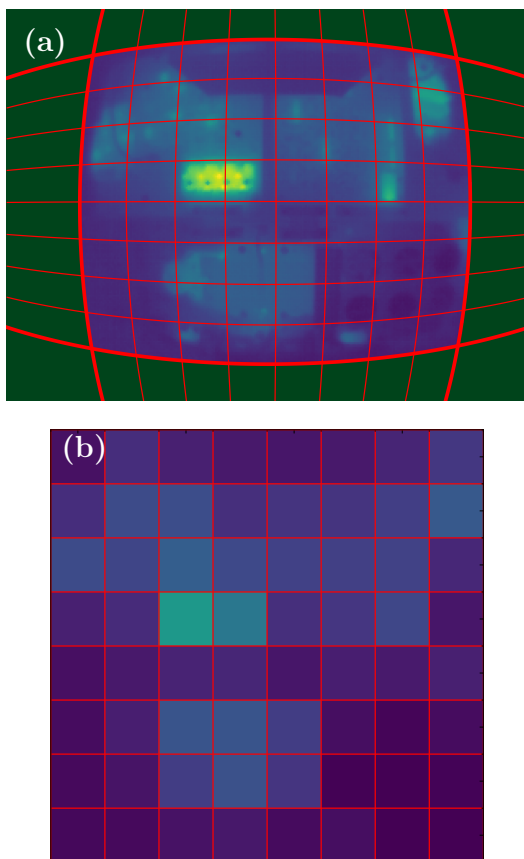


Figure 2: Image processing of the original image (a) and the results of averaging blocks to 8x8 image (b). The green shaded area in (a) represent the area outside of the power supply boundaries, which is used to estimate the room temperature

Training Results

We consider the use of Long-Short-Term-Memory (LSTM) networks to predict the temperature in the desired pixels. The choice of the LSTM network is due to its simplicity as well as performance in sequential data when compared

to other Recurrent Neural Networks (RNNs) [7]. Moreover, earlier studies using LSTMs on the internal sensors of the power supply showed promising results [5]. The LSTM model is trained to predict a sequence of length N , which represents N seconds. Training sought to minimize the Mean-Squared-Error (MSE) between the actual and predicted temperature ΔT distributions.

We started with a simple model using one LSTM layer to predict a single pixel; this pixel could represent any desired location in the power supply (e.g., heat sink or capacitor). Following that, we attempted to increase the number of pixels that the model needs to predict. Whenever we found that the simple model did not perform as expected, we attempted to increase the complexity of the model by increasing the number of cells in the LSTM layer n or adding more layers to the model. As the model became more complex, we used different optimization techniques to optimize the hyperparameter space [8]. During the training and validation, losses and accuracy were tracked to assess the performance of the model. However, the final assessment was based on the ability to detect anomalies using the test data, which contained synthetic anomalies.

An anomaly is declared for a pixel when the difference between the predicted and actual temperatures exceeds the chosen threshold for a chosen consecutive amount of time. A true positive is declared when the model detects an anomaly that overlaps with a true anomaly. If the detected anomaly does not overlap with a true anomaly, a false positive is declared. Positive rates (true and false positives) represent the precision of our model. Similarly, if an anomaly is present and the model fails to detect it, a false negative is declared, while non-anomalous data that are predicted by the model as normal are marked as true negatives. In our case, we consider a false negative to be the most expensive case, since undetected faults have the potential to cause facility downtime; false positives, on the other hand, are less of a concern in that evaluation by a technician is relatively quick.

The positive and negative rates are calculated for different thresholds, which are then used to compute the Precision-Recall (P-R) Curves. The P-R curves are calculated for each model and compared with each other; the result of such comparison is depicted in figure 3. The P-R curve shows very similar behavior for fewer than 16 pixels. However, for larger numbers of pixels, the model gradually lost performance and increasing the complexity of the model did not improve the P-R curve. The Area Under the Curve (AUC, ideally 1), for the 64-pixel model as ~ 0.70 , while for all other models the AUC was ~ 0.90 . The 64-pixel model's predictions are illustrated in Fig. 4.

DISCUSSION

LSTM networks can predict temperature variations in power supplies to great accuracy, making them a great candidate for anomaly detection in power supplies as well as other accelerator components with sequential data. Although the 64 pixel model performance is still not comparable to the

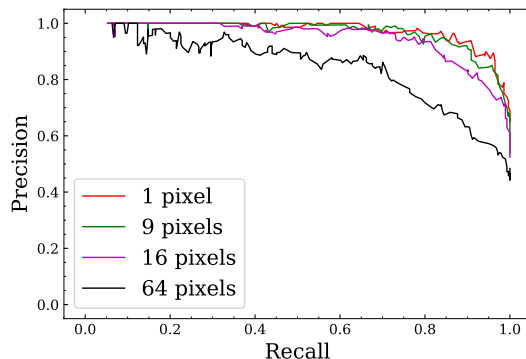


Figure 3: Precision-Recall curves for different LSTM models. The AUC for the 1,9,16 and 64 pixels models are 0.91,0.90,0.84 and 0.71, respectively.

lower pixel models in terms of P-R and AUC, the model is still able to predict the overall temperature variation across the power supply segments; see Fig. 4. However, larger errors are observed in pixels where temperature variation is low, e.g., around the edges. Moreover, the large variation of the response of different pixels to the same current change ΔI increases the complexity of the model. In terms of training, we found that larger LSTM models require very fine hyperparameter tuning. The tuning is typically done by a separate optimization that requires training for several iterations. This process takes much longer than the single pixel model, which takes 30 minutes to train on the same workstation.

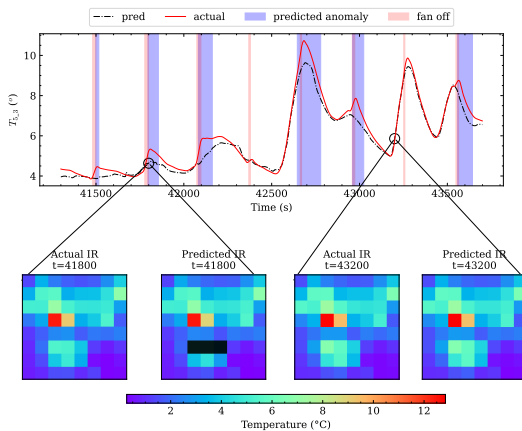


Figure 4: Predicted IR image based on the 64 pixel model. The top plot shows the predicted temperature (black dashed) and actual temperature (solid red). The blue and red shaded areas are predicted anomalies regions and regions were the fan was off, respectively. The four images below show the actual and predicted IR images at 2 different time steps

CONCLUSION AND OUTLOOK

The current work in predicting a smaller number of pixels, as well as previous work on predicting temperature from internal power supply sensors, are both encouraging. Indeed,

it is unclear that use of a large number of pixels is necessary, in that the goal is to detect temperature anomalies that are not detected by on-component sensors. If an anomaly is detected, human examination with a high-resolution camera would be undertaken to verify that an issue is present.

Subsequently, during the start-up of this APS-U run, we took data from a single sector of the APS-U storage ring fast corrector power supplies. The data acquisition was performed using the same steps mentioned for the power supply test stand. However, unlike the test stand, the power supplies in the storage ring do not have ambient temperature sensors, which makes accounting for external temperature variation difficult. Earlier work has shown that predicting the temperature difference between the internal sensors can help with this issue. The training and prediction results show similar behavior to the single pixel model of the test stand; Fig. 5. To compute this curve, anomalies were injected into the test data. These anomalies were analytically inserted with different locations and amplitude using a pseudo-random generator.

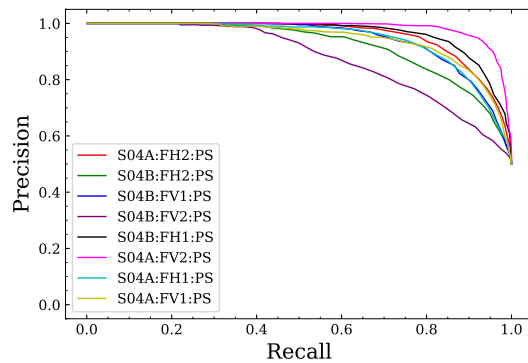


Figure 5: Precision-Recall curve for power supply in sector 04 in the APS-U.

The next step would involve taking similar data for all the APS-U fast correctors. Following that, an anomaly detection app based on the training results can be established where non-experts can inspect the results of the anomaly analysis. In parallel, we will seek to improve the 64-pixel model using the IR camera; different ML models will be tested, and their performance will be compared to the current LSTM model. Finally, these methods can be scaled to different types of power supplies, e.g., uni-polar and ramping supplies in the storage ring or the injector. Eventually, if the method proves itself in such tests, we will develop a plan to install IR sensors or low-resolution cameras inside operational power supplies.

ACKNOWLEDGMENT

We gratefully acknowledge the computing resources provided on Swing, a high-performance computing cluster operated by the Laboratory Computing Resource Center at Argonne National Laboratory. We are thankful for the help we received from the power supply group at the APS to perform this work.

REFERENCES

- [1] M. Borland *et al.*, “The upgrade of the Advanced Photon Source”, in *Proc. IPAC’18*, Vancouver, Canada, Apr.-May 2018, pp. 2872–2877.
doi:10.18429/JACoW-IPAC2018-THXGBD1
- [2] V. Sajaev *et al.*, “APS upgrade: Commissioning the world’s first light source based on swap-out injection”, presented at NAPAC’25, Sacramento, CA, USA, Aug. 2025, paper MOXP02, these proceedings.
- [3] A. Hillman, J. Carwardine, and G. Sprau, “Magnet power supply reliability at the advanced photon source”, *IEEE Conf. Part. Accel.*, vol. 5, pp. 3657–3659, 2001.
doi:10.1109/PAC.2001.988210
- [4] J. Wang, I. A. Abid, R. T. Keane, and G. S. Sprau, “Preliminary designs and test results of bipolar power supplies for APS Upgrade Storage Ring”, in *Proc. IPAC’18*, Vancouver, Canada, Apr.-May 2018, pp. 2381–2383.
doi:10.18429/JACoW-IPAC2018-WEPMF008
- [5] I. Lobach and M. Borland, “Recurrent neural networks for anomaly detection in magnet power supplies of particle accelerators”, *Mach. Learn. Appl.*, vol. 18, p. 100585, 2024.
doi:10.1016/j.mlwa.2024.100585
- [6] *S314HPX High Temp Starter Kit*, 320 x 240, 35HFOV, FF, <https://shop.thermal.com/S314HPX>, [Accessed 07-08-2025].
- [7] R. Khaldi, A. El Afia, R. Chiheb, and S. Tabik, “What is the best rnn-cell structure to forecast each time series behavior?”, *Expert Syst. Appl.*, vol. 215, p. 119140, 2023.
doi:10.1016/j.eswa.2022.119140
- [8] T. Akiba, S. Sano, T. Yanase, T. Ohta, and M. Koyama, “Op-tuna: A next-generation hyperparameter optimization framework”, in *Proc. 25th ACM SIGKDD Int. Conf. on Knowledge Discovery and Data Mining*, Anchorage, AK, USA, Aug. 2019.
doi:10.1145/3292500.3330701